

method is based upon the use of a wave function which describes the unstable state. This wave function is normalized and localized in coordinate space, although it has a rather slowly decaying exponential tail. All integrals appearing in the DWBA analysis are convergent, and special convergence factors as proposed by Huby and Mines are unnecessary. Furthermore, the resonant-state wave function is as easy to obtain as the bound-state wave function typically used in DWBA analysis. There is no need to integrate the cross section over the unobserved energy of the resonating pair as in the Vincent-Fortune method because this is already accomplished by the reso-

nant wave function.

Our method for DWBA analysis for scattering to resonant states has the further advantage that it is quite easy to apply. Indeed, existing DWBA codes may be used for such processes simply by substituting the resonant-state wave function for the usual bound-state wave function which appears in the description of the final state. We believe the present method will greatly facilitate the practical analysis of experiments of this type.

ACKNOWLEDGMENT

We are grateful to F. Coester for several helpful suggestions.

¹F. Coester and L. Schlessinger (to be published).

²C. M. Vincent and H. T. Fortune, *Phys. Rev. C* **2**, 782 (1970).

³R. Huby and J. R. Mines, *Rev. Mod. Phys.* **37**, 406 (1965).

⁴R. Huby, *Phys. Letters* **33B**, 323 (1970).

⁵B. J. Cole, R. Huby, and J. R. Mines, *Phys. Letters* **33B**, 320 (1970).

⁶L. Hulthen and M. Sugawara, in *Encyclopedia of Physics*, edited by S. Flugge (Springer, Berlin, 1957), Vol. 39.

⁷G. L. Payne and P. L. Von Behren, *Phys. Rev. C*

5, 1955 (1972).

⁸J. L. Alty, L. L. Green, R. Huby, G. D. Jones, J. R. Mines, and J. F. Sharpey-Schafer, *Nucl. Phys.* **A97**, 541 (1967).

⁹R. G. Newton, *Scattering Theory of Particles and Waves* (McGraw-Hill, New York, 1967).

¹⁰M. L. Goldberger and K. M. Watson, *Collision Theory* (Wiley, New York, 1964), p. 202.

¹¹M. Abramowitz and I. A. Stegun, *Handbook of Mathematical Functions* (National Bureau of Standards, Washington, D. C., 1965).

Nonlocal and Majorana Exchange Terms in the Optical Model*

G. W. Greenlees, W. Makofske,[†] Y. C. Tang, and D. R. Thompson
School of Physics, University of Minnesota, Minneapolis, Minnesota 55455
 (Received 12 June 1972)

The suggestion that nonlocal terms arising from the effects of antisymmetrization in light systems should be present in heavier systems, is examined. The introduction of one such term into the optical potential for proton-nucleus scattering produces significant effects at backward angles. It is shown that these nonlocal effects can be represented almost exactly by the introduction of a Majorana component into the real central potential. The results are applied in an analysis of 30-MeV proton elastic scattering data from ⁴⁰Ca.

I. INTRODUCTION

In a recent publication,¹ Greenlees and Tang (GT) discussed the need for nonlocal terms in optical-model potentials. Such terms are necessary to simulate the effects of antisymmetrization, which are not included explicitly in standard optical-model calculations. Studies of few-nucleon systems, where antisymmetrization is correctly included,² have shown that nonlocal potentials arise quite naturally and, as pointed out by GT, similar

terms should be present also in heavier systems. In practice it is rather difficult to antisymmetrize in these heavier systems explicitly and the results of studies on the light systems are used as a guide when choosing the appropriate form for the nonlocal potential for use in such cases.³

The present paper investigates further the effects of one particular nonlocal term in the potential. It is shown that this term can have a significant effect on the large-angle scattering amplitude, and may indeed be needed to represent

simultaneously elastic differential cross section and polarization data. The possibility of constructing a local potential which simulates the effects of the nonlocal one, is examined. The Born-approximation results of GT are modified and it is found that a local potential, with a Majorana component, is closely equivalent to the nonlocal potential.

Finally, 30 MeV $p + {}^{40}\text{Ca}$ elastic scattering cross section and polarization data are examined using a local potential with a Majorana space-exchange component. It is found that the inclusion of this component yields improved agreement with the experimental data. When accurate data at the extreme backward angles become available, it should be possible to determine the magnitude of the space-exchange component reasonably accurately.

II. FORMULATION

A. Nonlocal Potential

One-channel resonating-group calculations² which employ a central nucleon-nucleon potential have shown that, when antisymmetrization is explicitly included, the equation for the function $F(\vec{r})$ which describes the relative motion of two light nuclei, one or both with spin zero, is given by

$$\left[\frac{\hbar^2}{2\mu} \nabla^2 - V_D(r) - V_C(r) + E \right] F(\vec{r}) = \int K(\vec{r}, \vec{r}') F(\vec{r}') d\vec{r}' . \quad (1)$$

In Eq. (1), V_D is the direct nuclear potential, μ is the reduced mass, E is the relative energy in the c.m. system, and V_C is the direct Coulomb potential. The kernel function $K(\vec{r}, \vec{r}')$ contains terms of the form

$$K_1(\vec{r}, \vec{r}') = g_1(r, r') \exp[-\beta_1(\vec{r} - \vec{r}')^2] \quad (2)$$

and

$$K_2(\vec{r}, \vec{r}') = g_2(r, r') \exp[-\beta_2(\vec{r} + \vec{r}')^2], \quad (3)$$

where g_1 and g_2 are form factors, symmetric in r and r' , and β_1 and β_2 are nonlocal range parameters. As has been shown,² the V_D term in Eq. (1) arises from a folding of the spin- and isospin-independent part of the free nucleon-nucleon potential with the mass distributions of the particles and has been used by Greenlees, Pyle, and Tang⁴ as the real central part of the potential for the local optical model.

It was pointed out by GT that the K_1 kernel affects mainly the scattering amplitude at forward angles, while the K_2 term influences mainly the behavior at backward angles. Since the direct potential V_D yields a large forward-angle scattering amplitude, it may be quite difficult to study the

effects of K_1 . Therefore the present paper limits the study of nonlocal potentials to terms of the K_2 type, since the effects of such terms should not be screened so severely by V_D .

The form factor for K_2 is chosen to be a Gaussian function, symmetric in r and r' , given by:

$$g_2 = -g_{20} \exp[-\alpha_2(r^2 + r'^2)]. \quad (4)$$

With this choice for g_2 , the form of the nonlocal kernel is then:

$$K_2(\vec{r}, \vec{r}') = -g_{20} \exp[-\alpha(r^2 + r'^2)] \exp[-\beta(\vec{r} + \vec{r}')^2]. \quad (5)$$

In Eq. (5) the subscripts have been deleted from α and β , since the K_1 kernel will not be considered further here.

The kernel K_2 contains three parameters g_{20} , α , and β . However, it is not expected that the nonlocality range β will change significantly from nucleus to nucleus. It is therefore taken to be $\beta = 0.25 \text{ fm}^{-2}$, which is about the value found in resonating-group calculations of $n + {}^4\text{He}$ scattering.² Also, the value of α is clearly related to the size of the target nucleus. Later in this paper, an analysis of $p + {}^{40}\text{Ca}$ scattering data is presented; α is therefore chosen to be 0.06 fm^{-2} which, in Born approximation, yields a rms radius for the equivalent local potential about equal to the proton rms radius of ${}^{40}\text{Ca}$. It turns out that the results presented here are not very sensitive to the present choice of α and β . Having fixed α and β , the strength of the nonlocality g_{20} remains as the single free parameter.

To examine the effects of introducing a nonlocal term of the form K_2 [Eq. (5)] into the potential describing $p + {}^{40}\text{Ca}$ elastic scattering, Eq. (1) needs to be modified to take account of the presence of nonelastic channels and spin-orbit effects. This is normally done in the local approximation ($K=0$) by introducing an imaginary-potential term $iW_I(r)$ and a spin-orbit potential term $V_{so}(\vec{r}, \vec{\sigma})$ into the left-hand side of Eq. (1). The real terms V_D and V_{so} can be obtained by using folding procedures,⁴ or replaced by Woods-Saxon- and Thomas-form phenomenological potentials as in standard optical-model calculations; both methods give a reasonable representation of data at 30 MeV, especially at forward angles and for heavy nuclei. In the present analysis, the second approach was used to economize on the computing periods required, and the $p + {}^{40}\text{Ca}$ local optical-model potentials of Hnizdo *et al.*⁵ were used in Eq. (1). With this change, and using K_2 [Eq. (5)] for K , Eq. (1) was solved numerically for different values of g_{20} . The results for $g_{20} = 0.3, 0, \text{ and } -0.3 \text{ MeV fm}^{-3}$ are shown in Fig. 1. This figure shows that

a nonlocal kernel of the form of K_2 [Eq. (5)] has a significant effect on the elastic scattering in the backward hemisphere, particularly at angles beyond 120° . Forward of 100° , the predictions are little affected by variations in g_{20} . The scattering in this forward-angle region is dominated by the V_D term. Thus when data are being analyzed which include measurements at large angles, the inclusion of a nonlocal term of the K_2 type may be essential in obtaining a satisfactory description of the data.

B. Equivalent Local Potential

Since solving the integrodifferential equation [Eq. (1)] involves lengthy computing periods, an investigation was made into the possibility of constructing a local potential which reproduces the same effects as the nonlocal term discussed above.

In the context of the Born approximation, the scattering amplitude corresponding to the K_2 kernel can be written as

$$f_2 = \frac{-\mu}{2\pi\hbar^2} \int \exp(-i\vec{k}_f \cdot \vec{r}) K_2(\vec{r}, \vec{r}') \exp(i\vec{k}_i \cdot \vec{r}') d\vec{r} d\vec{r}', \quad (6)$$

where \vec{k}_i and \vec{k}_f are the initial and final wave vectors. Substituting Eq. (5) into Eq. (6) and integrating, yields

$$f_2 = \frac{\mu}{2\pi\hbar^2} g_{20} \left[\frac{\pi^2}{\alpha(\alpha+2\beta)} \right]^{3/2} \exp\left[\frac{-k^2}{2\alpha+4\beta} \right] \times \exp\left[\frac{-\beta k^2}{\alpha(\alpha+2\beta)} \cos^2 \frac{\theta}{2} \right], \quad (7)$$

with $|\vec{k}_i| = |\vec{k}_f| = k$ and θ being the scattering angle. Equation (7) shows that f_2 increases monotonically as a function of θ .

In the Born approximation, f_2 is also the scattering amplitude of the local potential:

$$V_2 = -g_{20} \left(\frac{\pi}{\beta} \right)^{3/2} \exp\left[-\frac{k^2}{2(\alpha+2\beta)} \right] \times \exp\left[-\frac{\alpha}{\beta} (\alpha+2\beta)r^2 \right] P^r. \quad (8)$$

This expression for V_2 contains a Majorana exchange operator P^r , which interchanges the position coordinates of the target and the incident particle.⁶ This operation introduces an odd-even orbital angular momentum dependence and any local potential which yields features similar to the nonlocal K_2 potential in a scattering calculation, would be expected to include this operator. Thus, a simple way of introducing such a feature into the usual local optical-model potential is to multiply the real central part by a factor $(1+C_R P^r)$.

The local optical-model potential of Ref. 5, used

in Sec. IIA with the nonlocal kernel, was therefore modified by including the factor $(1+C_R P^r)$ in the real central term and the scattering was computed using this new local potential with $K_2=0$. The coefficient C_R was varied and a comparison made with the nonlocal calculations of Sec. IIA. The

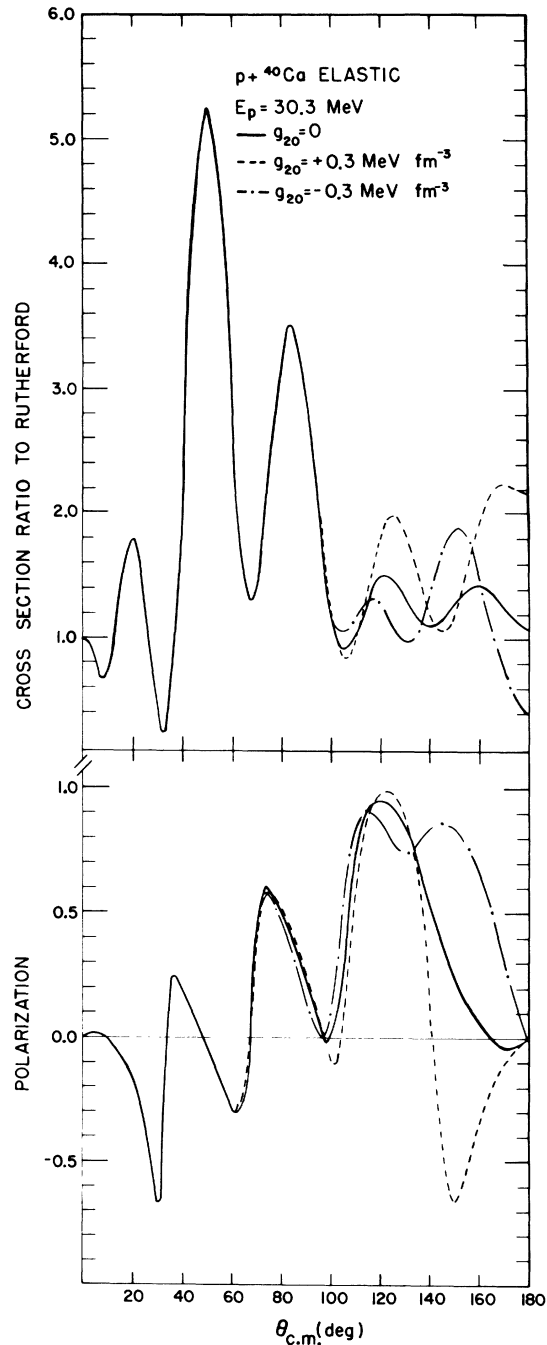


FIG. 1. The dependence of elastic scattering predictions on the magnitude, g_{20} , of the nonlocality term $K_2(\vec{r}, \vec{r}')$.

results are shown in Fig. 2, where the solid curve corresponds to the nonlocal calculation with $g_{20} = -0.3 \text{ MeV fm}^{-3}$ and the dashed curve to the local calculation with $C_R = -0.01$. The agreement between the two sets of predictions is very good and suggests that, at least at the present stage of development, a local odd-even potential of the form $V_D(r)C_R P^r$, gives an adequate representation of a nonlocal kernel of the K_2 type. In general, it was found that the strength coefficients of the two descriptions are related by $C_R = a g_{20}$ with $a \approx 0.033 \text{ MeV}^{-1} \text{ fm}^3$.

The close equivalence of the local and nonlocal calculations shown in Fig. 2 is somewhat surprising, since the choice of the local form was made upon the basis of simplicity and Born-approximation arguments. For 30-MeV protons scattered by ^{40}Ca , Born-approximation calculations are not expected to provide a good description of the interaction. It is therefore interesting to examine the present result in more detail.

Substitution of the appropriate constants for the 30 MeV $p + ^{40}\text{Ca}$ case ($\alpha = 0.06 \text{ fm}^{-2}$, $\beta = 0.25 \text{ fm}^{-2}$, $k = 1.18 \text{ fm}^{-1}$) into Eq. (8) with g_{20} in MeV fm^{-3} and r in fm gives

$$V_2 = -12.7 g_{20} e^{-0.135r^2} P^r \text{ MeV}. \quad (9)$$

The volume integral of this potential is $I_2 = 1420 g_{20} \text{ MeV fm}^3$. The volume integral of the real central potential for $p + ^{40}\text{Ca}$ taken from Ref. 5 is $16\,400 \text{ MeV fm}^3$ and the corresponding Majorana local component would have a volume integral $16\,400 C_R \text{ MeV fm}^3$. Equating the Born-approximation nonlocal term and the local equivalent odd-even term, via the volume integrals, gives $a = 0.087 \text{ MeV}^{-1} \text{ fm}^3$ compared to the value $0.033 \text{ MeV}^{-1} \text{ fm}^3$ obtained previously. However, the derivation of Eq. (9) used the incident proton energy (30 MeV) to obtain k ; a more appropriate choice might be the wave number in the interaction region, or approximately, the value at the half-way point of the local real central potential. The volume integral I_2 was therefore recalculated using this recipe, yielding a value $493 g_{20} \text{ MeV fm}^3$. This value of I_2 gives $a = 0.03 \text{ MeV}^{-1} \text{ fm}^3$, in close agreement with the value obtained by comparison of the angular distributions (Fig. 2).

Use of the actual local wave number, rather than that corresponding to the energy E , is done more exactly by writing Eq. (8) as⁷:

$$V_2^{MB} = U_2 P^r = -g_{20} \left(\frac{\pi}{\beta} \right)^{3/2} \exp \left[-\frac{\mu}{\hbar^2} \frac{E - V_D(r) - V_C(r)}{\alpha + 2\beta} \right] \times \exp \left[-\frac{\alpha}{\beta} (\alpha + 2\beta) r^2 \right] P^r, \quad (10)$$

where

$$V_D(r) = V \{ 1 + \exp[(r - r_R A^{1/3})/a_R] \}^{-1}, \quad (11)$$

with $V = -47.3 \text{ MeV}$, $r_R = 1.158 \text{ fm}$, and $a_R = 0.74 \text{ fm}$ (Ref. 5). The function U_2 is plotted in Fig. 3 using $g_{20} = -0.3 \text{ MeV fm}^{-3}$ along with $C_R V_D(r)$ using

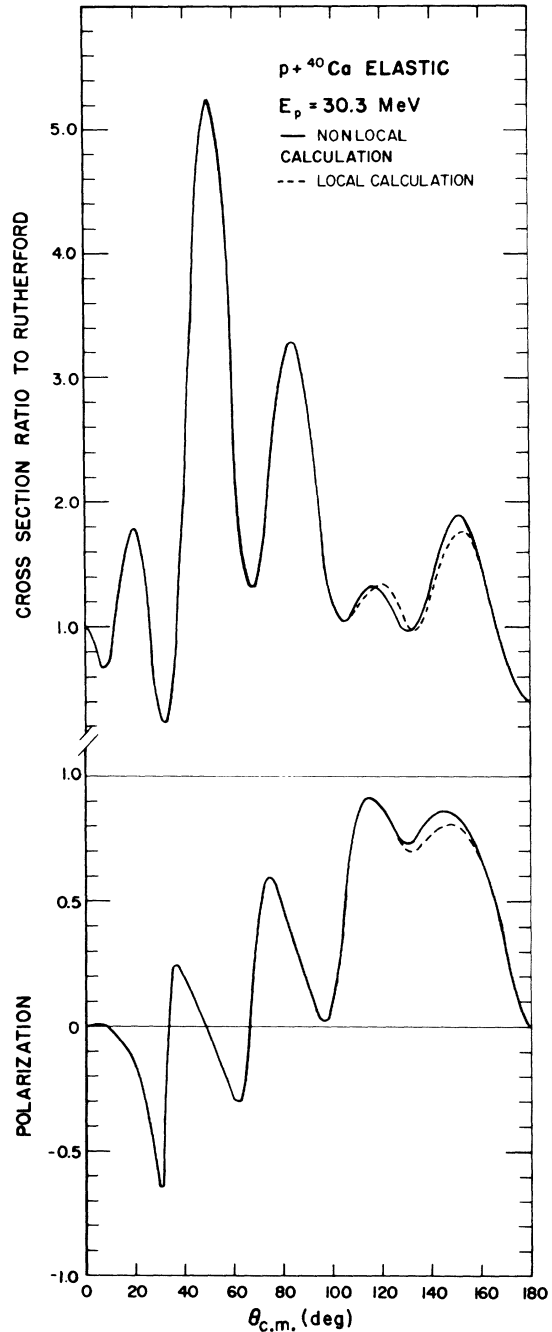


FIG. 2. Comparison of predictions obtained using a nonlocal kernel, $K_2(\vec{r}, \vec{r}')$, with $g_{20} = -0.3 \text{ MeV fm}^{-3}$ and a local Majorana term with $C_R = -0.01$.

$C_R = -0.01$. The agreement between the two potentials in the important surface region, $r > 2$ fm, is quite close. It is known that in the elastic scattering of protons at 30 MeV the detailed shape of the real central potential is not critical, the well-defined quantities being the volume integral and the mean square radius of the potential.⁸ For the potentials of Fig. 3 these quantities are 173 MeV fm³ and 16.4 fm² for U_2 , and 164 MeV fm³ and 16.9 fm² for $C_R V_D(r)$. This agreement is similar to the agreement found for different central potentials which give equivalent fits to data in conventional optical-model calculations ($\pm 4\%$ for the volume integral and $\pm 4\%$ for the mean square radius.) These considerations lend some justification to the equivalence found between the odd-even local and the nonlocal calculations [Fig. (2)].

III. COMPARISON WITH DATA

It is evident from Fig. 1 that a nonlocality of the form of K_2 , with a volume integral about 1% of that of the local potential, produces significant effects only at large scattering angles. Therefore, it is essential that measurements at large angles be available if an analysis of data is to yield useful information concerning K_2 . Furthermore, local potentials used to describe detailed elastic scattering data, generally include 8–10 parameters; this allows considerable flexibility, when fitting data, to compensate at least partially for relatively small effects not included in the local

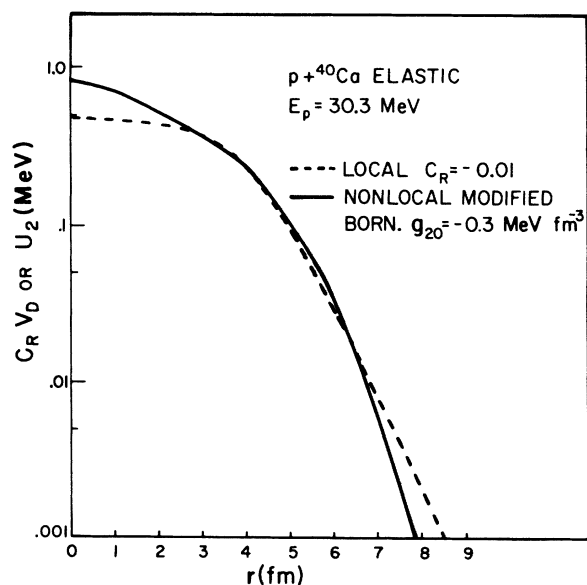


FIG. 3. The radial dependence of potentials, $C_R V_D$ and V_2 , given by: (a) a local Majorana term; and (b) a non-local K_2 term, evaluated using the modified Born-approximation method described in the text.

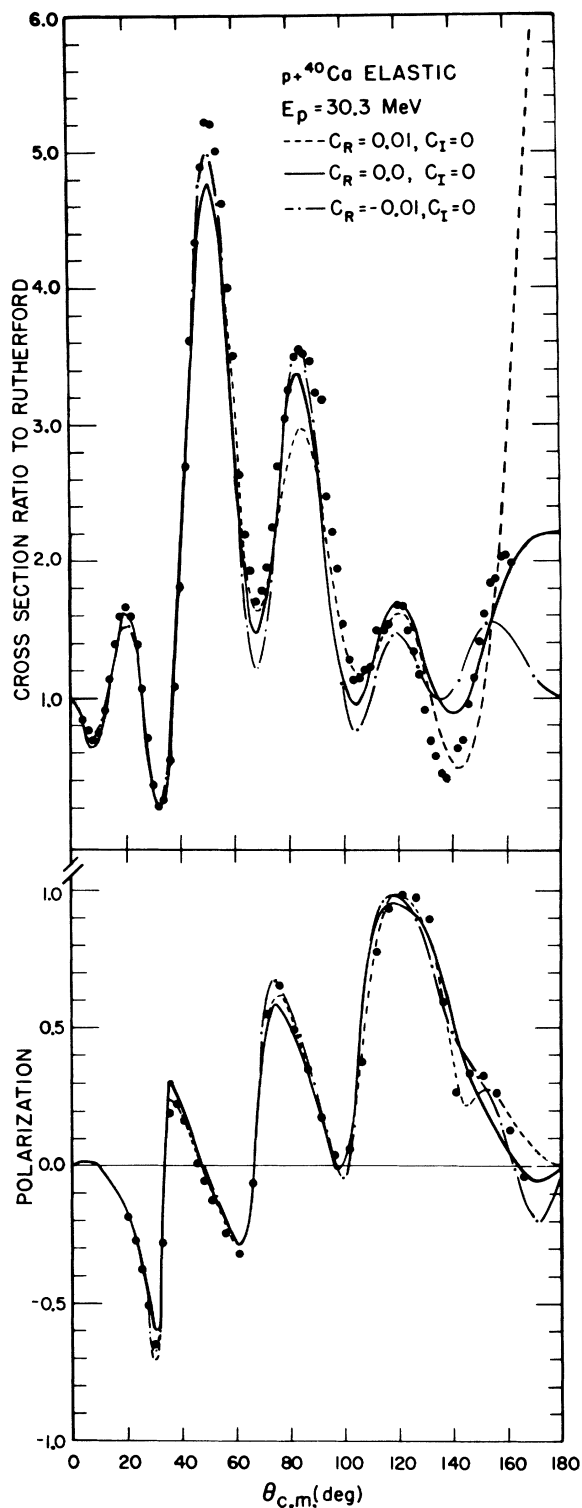


FIG. 4. Comparison, with data, of predictions obtained for fixed values of C_R , the real-central-potential Majorana coefficient, and by searching on all other parameters. The imaginary-potential Majorana coefficient, C_I , was set equal to zero.

potential model. Any such effects are likely to be most evident at large angles where the direct and Coulomb scattering have their smallest amplitudes.

In the present case, accurate data for both differential cross sections and polarization out to angles close to 180° are desirable. The proton energy should be high enough to avoid compound elastic effects and the target mass number should not be too high, since the importance of K_2 is expected to diminish as the size of the system increases. Existing data which most closely meet these criteria are for 30.3-MeV protons scattered by ^{40}Ca where accurate differential-cross-section measurements⁹ are available from 4° to 162° and accurate polarization measurements⁵ from 20° to 165° . An optical-model analysis of these data using local potentials,⁵ experienced some difficulty in obtaining a good representation of the data at the larger scattering angles.

The initial analysis of these ^{40}Ca data was performed using a local potential of the form used in Ref. 5 along with an odd-even l feature in the strength of the real central potential. The equation to be solved takes the form

$$\left[\frac{\hbar^2}{2\mu} \nabla^2 - V_D(r)(1 + C_R P^r) - iW_I(r) - V_{so}(\vec{r}, \vec{\sigma}) - V_C(r) + E \right] F(\vec{r}, s) = 0, \quad (12)$$

where

$$\begin{aligned} V_D(r) &= Vf(r, r_R, a_R), \\ V_{so} &= V_s \left(\frac{\hbar}{m\pi c} \right)^2 r^{-1} f'(r, r_s, a_s), \\ W_I(r) &= W_V f(r, r_I, a_I) - 4a_I W_D f'(r, r_I, a_I), \end{aligned} \quad (13)$$

with

$$f(r, r_0, a_0) = \{1 + \exp[(r - r_0 A^{1/3})/a_0]\}^{-1}. \quad (14)$$

The Coulomb potential $V_C(r)$ is that due to a uniform charge distribution with a spatial distribution $f(r, r_C, a_C)$ with $r_C = 1.11$ fm and $a_C = 0.502$ fm.

Using as starting values those given in Ref. 5, the parameters V , r_R , a_R , W_V , W_D , r_I , a_I , V_S , r_S , and a_S were varied to find a minimum in χ^2 defined by:

$$\chi^2 = \frac{1}{N} \sum_{i=1}^N \left[\frac{q_{th}(\theta_i) - q_{exp}(\theta_i)}{q_{error}(\theta_i)} \right]^2, \quad (15)$$

where $q_{th}(\theta_i)$ and $q_{exp}(\theta_i)$ are the theoretical and ex-

perimental quantities at scattering angle θ_i , respectively, and $q_{error}(\theta_i)$ is the associated experimental error.¹⁰ Such searches were performed for a range of values of C_R , the Majorana coefficient. The model predictions for $C_R = -0.01$, 0, and $+0.01$ are shown in Fig. 4 along with the experimental data points. These results do not seem to provide convincing evidence of the need for a finite C_R in the model. Thus, while $C_R = +0.01$ produces improvement in the valley region around 140° in the cross-section curve and reproduces the subsidiary peak in $P(\theta)$ at 150° , it considerably worsens the cross-section representation of the peak around 85° and produces a large peak at 180° in contradiction to the trend implied by the last few measured points. On the other hand, $C_R = -0.01$ fails to reproduce the cross section dip at 140° and the subsidiary peak in $P(\theta)$ at 150° , but improves the representation of the cross section (50 and 85°) and polarization (35 and 75°) maxima, and has a more reasonable behavior beyond 165° . It is clear that even with the inclusion of a Majorana component in the real central potential, not all features of the scattering are being represented by the model and that various compromises are possible in the parameter space.

The need for a Majorana component in the real potential was postulated by analogy with the results of one-channel calculations for few-nucleon systems. The success of these calculations diminishes with increasing energy as more reaction channels become operative. In such cases it has been found that the introduction of an imaginary potential with a Majorana exchange component, considerably improves the description of data at higher energies.¹¹ In the analysis of the elastic scattering of systems such as $p + ^{40}\text{Ca}$, the need for an imaginary potential in the local optical model is well established. Furthermore, quite general arguments suggest that both the real and imaginary optical potentials are nonlocal.¹² It was decided, therefore, to examine the consequences of introducing a Majorana exchange component into the imaginary potential of Eq. (12). Thus, $W_I(r)$ in that equation was multiplied by a term $(1 + C_I P^r)$. The fitting of data proceeded as before with various combinations of fixed C_R and C_I . It was found to be relatively easy to determine C_I at values around -0.05 . The results of these calculations for C_R values of 0.01, 0, and -0.01 with optimum C_I values, are shown in Fig. 5. The representation of the data shown in Fig. 5 is considerably improved over that of Fig. 4 ($C_I = 0$); all the features of the data are being reproduced and the large angle behavior indicates a value for C_R between zero and -0.01 .

To obtain a better estimate of C_R , it is clearly

necessary to have measurements at angles beyond 170° . This point is illustrated in Fig. 6, where the magnitude of the observed to Rutherford cross section at 160° , 170° , and 180° is plotted as a

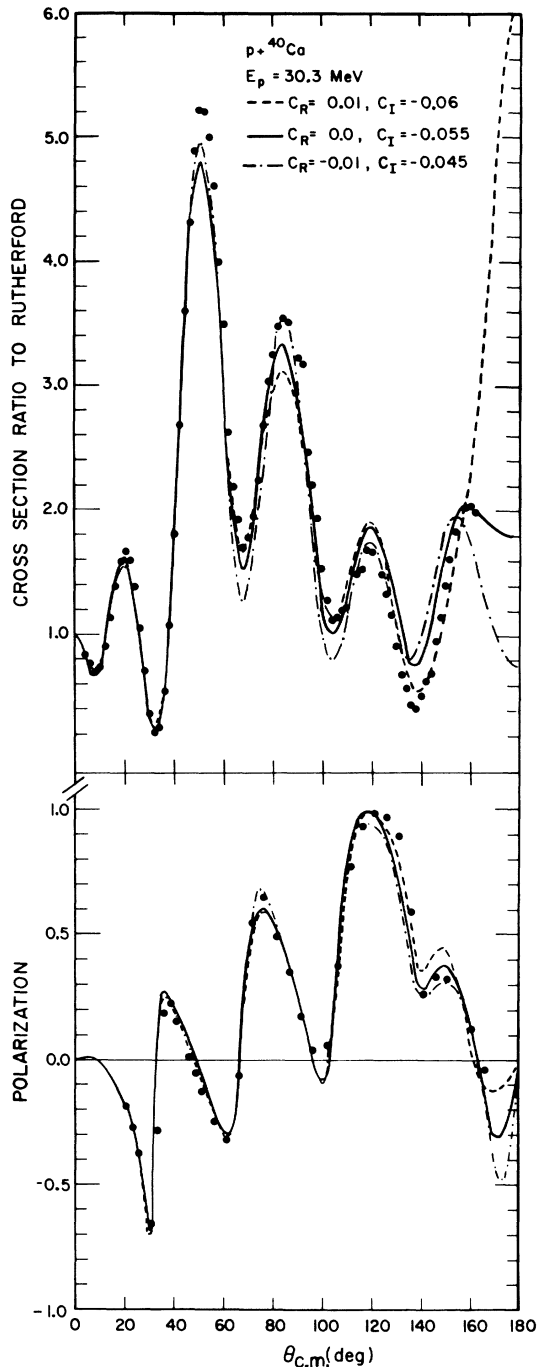


FIG. 5. Comparison, with data, of predictions obtained for fixed values of C_R , the real-central-potential Majorana coefficient, and by searching on all other parameters. The imaginary-potential Majorana coefficient, C_I , was fixed at its optimum value.

function of C_R . The variation with C_R in Fig. 6 increases markedly for 170° and 180° . If data were available at these large angles, for both the differential cross section and the polarization, it seems probable that the magnitude of the K_2 term (or its Majorana equivalent) could be determined.

Similar data to those used here for ^{40}Ca are also available for ^{58}Ni . In this latter case, the differential-cross-section measurements⁹ have been extended from 162° to 175° by Put, Urone, and Paans.¹³ In an analysis of differential cross section only, Put *et al.* found that the local optical-model analysis of Greenlees *et al.*¹⁴ of the previous data, gave a satisfactory description at the larger angles and concluded that the results presented no evidence for an exchange term of the form of K_2 . However, in the case of ^{58}Ni , the importance of this term is expected to be smaller than for ^{40}Ca because of the higher- A value. Furthermore, the present results (Fig. 4) show that it is important to analyze both cross-section and polarization data simultaneously, and even then, definitive conclusions are difficult to draw in the absence of an imaginary Majorana term. The results of Put *et al.* can, therefore, not be considered as conclusive.

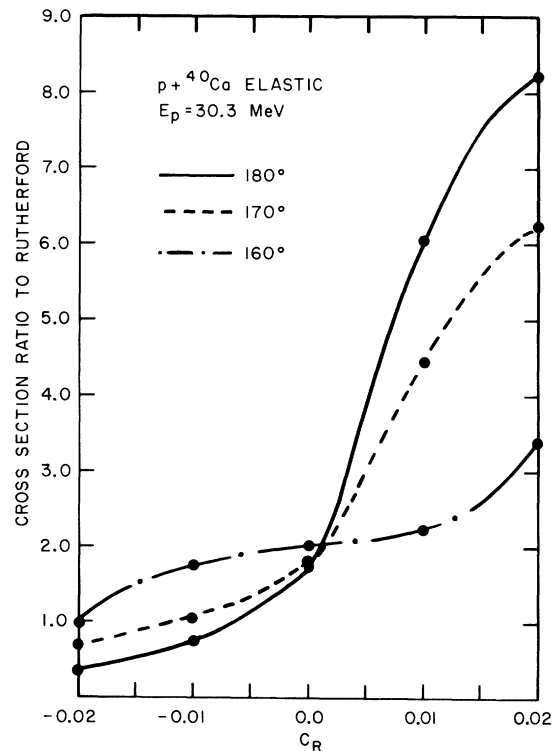


FIG. 6. The sensitivity of the large-angle cross section predictions to the value of C_R , using optimum values of C_I .

IV. CONCLUSION

The effects of introducing a nonlocal kernel into the optical model have been examined. A nonlocal contribution of seemingly small magnitude produces significant effects on the large-angle scattering amplitude. The form of the kernel was obtained from the results of antisymmetrized microscopic calculations for light systems and an almost exact equivalence was found using a local potential with a Majorana exchange feature. The effect of this component is to introduce an odd-even orbital angular momentum dependence into the local optical potential.

Existing data do not extend to large enough scattering angles to enable a thorough examination of the magnitude of the new term to be made. However, provided a similar odd-even feature is introduced into the phenomenological imaginary potential, a significant improvement is obtained in

the representation of $p + {}^{40}\text{Ca}$ scattering at 30 MeV, where data at angles up to 165° exists. The results indicate the additional term to have a volume integral of order 1% of the local central term. When accurate data for both differential cross section and polarization become available, at scattering angles greater than 170° , the importance of the nonlocality can be better determined.

Finally, it should be mentioned that antisymmetrization effects are expected to become more important as the atomic weight of the incident particle becomes closer to that of the target nucleus.² Thus, it is likely that these effects will manifest themselves in a significant manner in analyses of experimental data on heavy-ion scattering, such as the scattering of C^{12} on O^{16} .¹⁵ In these analyses, the inclusion of Majorana components in both the real and imaginary potentials may be an important step and should certainly be considered in the future.

*Work supported in part by the U. S. Atomic Energy Commission Contracts Nos. AT(11-1)-1265 and AT(11-1)-1764. This is report number COO-1265-119.

†Present address: Nevis Cyclotron Laboratories, Columbia University, Irvington, New York.

¹G. W. Greenlees and Y. C. Tang, *Phys. Letters* **34B**, 359 (1971).

²D. R. Thompson and Y. C. Tang, *Phys. Rev. C* **4**, 306 (1971); Y. C. Tang, in *Proceedings of the International Conference on Clustering Phenomena in Nuclei, Bochum, West Germany, 1969* (International Atomic Energy Agency, Vienna, Austria, 1969); Y. C. Tang and R. E. Brown, *Phys. Rev. C* **4**, 1979 (1971).

³Other authors have also discussed nonlocal corrections to the usual nucleon-nucleus optical potential as well as the construction of local effective potentials which simulate nonlocal effects. See, for example, the article by M. Coz *et al.*, *Ann. Phys. (N.Y.)* **58**, 504 (1970), and references contained therein.

⁴G. W. Greenlees, G. J. Pyle, and Y. C. Tang, *Phys. Rev.* **171**, 1115 (1968).

⁵V. Hnizdo, O. Karban, J. Lowe, G. W. Greenlees, and W. Makofske, *Phys. Rev. C* **3**, 1560 (1971).

⁶The operator P^r changes $F(\vec{r})$ into $F(-\vec{r})$; thus, it may be called a parity operator.

⁷The "modified Born" treatment presented here pro-

duces almost identical results to those obtained with an approximation procedure used by Perey and Buck [*Nucl. Phys.* **32**, 353 (1962)] in establishing an approximate equivalence between local and nonlocal potentials.

⁸G. W. Greenlees, W. Makofske, and G. J. Pyle, *Phys. Rev. C* **1**, 1145 (1970).

⁹B. W. Ridley and F. Turner, *Nucl. Phys.* **58**, 497 (1964).

¹⁰The errors quoted for the measured polarizations in Ref. 5 were increased to include, as a magnitude variation, the angular uncertainty $\pm 0.25^\circ$ present in the measurements and the new error values are used in Eq. (15). The calculated polarizations were averaged over the detector angular acceptance of $\pm 1.7^\circ$ ($\theta \geq 60^\circ$) and $\pm 1.5^\circ$ ($\theta < 60^\circ$) to obtain the theoretical values for Eq. (15).

¹¹D. R. Thompson, Y. C. Tang, and R. E. Brown, *Phys. Rev. C* **5**, 1939 (1972).

¹²H. C. Benöhr and K. Wildermuth, *Nucl. Phys.* **A128**, 1 (1969).

¹³L. W. Put, P. P. Urone, and A. M. J. Paans, *Phys. Letters* **35B**, 311 (1971).

¹⁴G. W. Greenlees, V. Hnizdo, O. Karban, J. Lowe, and W. Makofske, *Phys. Rev. C* **3**, 1063 (1970).

¹⁵R. H. Siemssen, in *Proceedings of the Symposium on Heavy-Ion Scattering*, Argonne National Laboratory, 1971, p. 145.